MTL TR 91-1

AD

(2)

TRANSIENT CRYSTALLIZATION OF AN AROMATIC POLYETHERIMIDE: EFFECT OF ANNEALING

C. RICHARD DESPER, ALEX J. HSIEH, and
NATHANIEL S. SCHNEIDER
POLYMER RESEARCH BRANCH

January 1991

US ARMY
LABORATORY COMMAND
MATERIALS TECHNOLOGY LABORATORY

U.S. ARMY MATERIALS TECHNOLOGY LABORATORY
Watertown, Massachusetts 02172-0001

The findings in this report are not to be construed as an official Department of the Army position, unless so designated by other authorized documents.

Mention of any trade names or manufacturers in this report shall not be construed as advertising nor as an official indorsement or approval of such products or companies by the United States Government.

DISPOSITION INSTRUCTIONS

Destroy this report when it is no longer needed.
Do not return it to the originator.

UNCLASSIFIED

SECURITY CLASSIFICATION OF THIS PAGE *(When Data Entered)*

REPORT DOCUMENTATION PAGE		READ INSTRUCTIONS BEFORE COMPLETING FORM
1. REPORT NUMBER MTL TR 91-1	2. GOVT ACCESSION NO.	3. RECIPIENT'S CATALOG NUMBER
4. TITLE *(and Subtitle)* TRANSIENT CRYSTALLIZATION OF AN AROMATIC POLYETHERIMIDE: EFFECT OF ANNEALING		5. TYPE OF REPORT & PERIOD COVERED Final Report 6. PERFORMING ORG. REPORT NUMBER
7. AUTHOR(s) C. Richard Desper, Alex J. Hsieh, and Nathaniel S. Schneider		8. CONTRACT OR GRANT NUMBER(s)
9. PERFORMING ORGANIZATION NAME AND ADDRESS U.S. Army Materials Technology Laboratory Watertown, Massachusetts 02172-0001 SLCMT-EMP		10. PROGRAM ELEMENT, PROJECT, TASK AREA & WORK UNIT NUMBERS D/A Project: 1L161102AH42
11. CONTROLLING OFFICE NAME AND ADDRESS U.S. Army Laboratory Command 2800 Powder Mill Road Adelphi, Maryland 20783-1145		12. REPORT DATE January 1991 13. NUMBER OF PAGES 17
14. MONITORING AGENCY NAME & ADDRESS *(if different from Controlling Office)*		15. SECURITY CLASS. *(of this report)* Unclassified 15a. DECLASSIFICATION/DOWNGRADING SCHEDULE

16. DISTRIBUTION STATEMENT *(of this Report)*

Approved for public release; distribution unlimited.

17. DISTRIBUTION STATEMENT *(of the abstract entered in Block 20, if different from Report)*

18. SUPPLEMENTARY NOTES

19. KEY WORDS *(Continue on reverse side if necessary and identify by block number)*

Polyetherimide
Crystallization
Annealing
Calorimetry
Phase transformation
Crystal structure
Polymers

20. ABSTRACT *(Continue on reverse side if necessary and identify by block number)*

(SEE REVERSE SIDE)

DD FORM 1 JAN 73 1473 EDITION OF 1 NOV 65 IS OBSOLETE

UNCLASSIFIED

SECURITY CLASSIFICATION OF THIS PAGE *(When Data Entered)*

Block No. 20

ABSTRACT

A systematic study using differential scanning calorimetry (DSC) has been performed on the annealing behavior of an aromatic polyetherimide (Ultem 5001). Although crystallization from the melt did not occur, crystallinity was easily induced in the presence of methylene chloride. With annealing, a sharp melt endotherm of the solvent-treated polyetherimide was observed. The melt temperature determined after annealing for 30 minutes increased progressively as the annealing temperature increased leading to an extrapolation to an apparent equilibrium melt temperature of 369°C. However, the melt temperature, as well as crystallinity, increased with the increase of the residence time at each annealing temperature. X-ray diffraction data revealed two distinct crystalline phases: a low temperature (alpha) phase obtained by crystallization for one-half hour at 248°C and 258°C, and a high temperature (beta) phase obtained at 258°C for three hours, or exceeding 258°C. Values of heat of fusion per gram of crystallite were consistent with a range 247 J/g to 261 J/g for the samples of higher crystallinity.

CONTENTS

INTRODUCTION

Solvent induced crystallization (SINC) has been well established in polycarbonate,[1-3] and polyethylene terephthalate.[4,5] Wilkes et al.[1] showed that well-developed spherulitic texture can be induced in polycarbonate by exposure to a nonreactive liquid or vaporous organic environment. In their studies using scanning electron microscopy (SEM), they also observed distinct plastic deformation of the induced spherulites in the polycarbonate samples which had been subjected to deformation at temperatures slightly above the glass transition temperature of 145°C.

Recently, several other SINC studies have been reported on high temperature thermoplastics including polyarylate,[6] polyimidesulfone,[7] polyetherimide,[8] poly(aryl ether ketone ketone) (PEKK),[9] LaRC-TPI (the NASA Langley Research Center-Thermoplastic Polyimide),[10-13] and a thermoplastic polyimide based on 4,4'-isophthaloyldiphthalic anhydride (IDPA) and 1,3-bis(4-amino-phenoxy-4'-benzoyl)benzene (1,3-BABB).[14] In the study of solvent crystallized polyarylate,[6] Berger showed a transition from shear deformation to crazing for an initially ductile amorphous material. PEKK, as pointed out by Avakian et al.,[9] displayed two different crystal structures after either exposure to methylene chloride vapor at room temperature or low temperature annealing. These crystal structures were different from those obtained by slow cooling from the melt or by high temperature annealing. Such behavior was not observed in poly(aryl ether ether ketone) (PEEK), which displayed only a single crystal form.[9] Crystallization which was attributed to the presence of residual solvent from processing also occurred in LARC-TPI.[10-13]

Ultem aromatic polyetherimide, first reported by Serfaty,[15] is an amorphous thermoplastic with the following structure for a commercially available Ultem 1000.

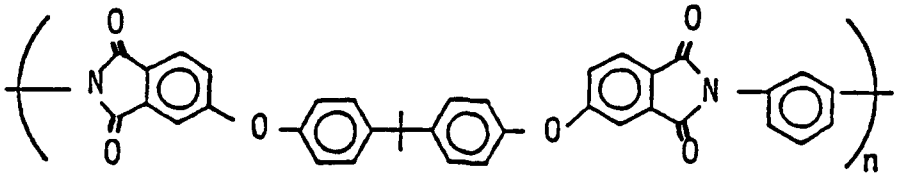

Our studies have been carried out on Ultem 5001-based materials which is a new aromatic polyetherimide with improved solvent resistance, but its chemical structure is not known in the literature. Results showed that crystallization occurred when the Ultem 5001 materials were exposed to methylene chloride.[16] Despite the original toughness, the solvent exposed polyetherimide film specimens became brittle. Although crystallization of Ultem 5001 polyetherimide can be easily induced in the presence of methylene chloride, attempts to achieve thermal crystallization in these materials have not yet been successful. Samples appear to be amorphous once exposed to a processing temperature above the melting point and do not appear to crystallize unless exposed to solvent.

The reluctance to crystallize from the melt in these high temperature polymers is partly due to the high viscosity of their melts. For example, LARC-TPI has a viscosity in the region of 10^5 - 10^6 Pa-s at approximately 100°C above T_g,[11] which is significantly higher than in conventional thermoplastics. As a result, crystallization from the melt is kinetically hindered and an amorphous, yet crystallizable, glass is formed upon cooling. However, the introduction of a good swelling agent will create sufficient mobility to allow the glass to crystallize.

The purpose of this report is to determine the effect of thermal history on the crystallization behavior of Ultem 5001 polyetherimide. Results of a systematic study using differential scanning calorimetry (DSC) on the annealing of solvent-treated polyetherimide are presented in this report. Degree of crystallinity as determined by wide angle X-ray diffraction, along with X-ray evidence for two different crystalline phases, are also included in this report.

EXPERIMENTAL

Ultem 5001 polyetherimide film was obtained from the General Electric Company. Experiments of solvent-induced crystallization were carried out in methylene chloride and in chloroform at room temperature. The solvent-treated films were then dried in vacuum for 24 hours. A dried sample, weighing 4 mg to 5 mg, was prepared in an aluminum pan for each annealing treatment which was carried out via a Perkin-Elmer DSC in a nitrogen atmosphere. Annealing temperatures of 248°C, 258°C, 268°C, 278°C, 287°C, and 297°C were chosen for this study. Thermal properties were determined via DSC, typically at a heating rate of 20°C/min.

Wide angle X-ray diffraction data were obtained with a T.E.C. model 210 position-sensitive detector mounted on a Picker four-circle goniostat using monochromatic radiation at 1.5418 Å and a Lecroy 3500 multiple-channel analyzer. A standard sealed copper anode X-ray tube was used at 40 kV and 20 mA. The thin film specimens from the DSC pans were mounted as transmission samples onto a metal disc sample holder, using cellophane tape (Scotch Brand Tape Core Series 2-4600). The detector, as configured, had a useful range of 20° in the Bragg angle 2θ. In order to obtain complete data for each specimen, three patterns were measured for each specimen: one centered at $2\theta = 22^{\circ}$, spanning $2\theta = 12^{\circ}$ to 32°; a second centered at $2\theta = 40^{\circ}$, spanning $2\theta = 30^{\circ}$ to 50°; and a third centered at $2\theta = 60^{\circ}$, spanning $2\theta = 50^{\circ}$ to 70°. A counting time of two hours was routinely used for the Ultem patterns. Since the cellophane tape also scattered X-rays, blank patterns of tape alone were measured then subtracted from the specimen patterns. The blank patterns proved to be amorphous with a single diffuse peak showing a maximum at $2\theta = 19^{\circ}$. The counting time for the blank patterns was lengthened to 19 hours to improve the precision of the blank subtraction process.

The X-ray diffraction patterns were transmitted from the diskette storage of the Lecroy 3500 multiple channel analyzer to a VAX (TM Digital Equipment Corporation) 11/730 computer for analysis. The data were subjected to three operations:

- The data were corrected for background (using the cellophane tape blank patterns).
- The Lorenz-polarization correction factor f_{LP} described by Alexander[17] was applied.
- Crystalline peaks evident in the data were curve-fit by a Marquardt iterative method[18] to determine peak parameters.

The second and third calculations are described more fully in the Appendix.

RESULTS AND DISCUSSION

Annealing Studies

Crystallization occurred immediately after Ultem 5001 films were exposed to liquid methylene chloride. The originally translucent films became completely opaque and brittle. A typical DSC thermogram, with a broad melting endotherm in the first heating scan up to 327°C,

is shown in Figure 1, Curve 1 for the methylene chloride exposed specimen; the peak of the endotherm is at 265°C. The sample was then quenched. Thereafter, a second heating scan was carried out, which displayed a glass transition temperature of 230°C without any melting endotherm, shown in Figure 1, Curve 2. This indicated that crystallites induced by methylene chloride exposure were completely removed by heating above the melt temperature. However, the first heating scan in Figure 1 shows no glass transition but a baseline shift after the endothermic peak. This can be partly due to an abnormally small increment between the glass transition temperature and the melt temperature, such that a very diffuse glass transition is masked by the melting of paracrystalline structure. Such a small temperature increment can also retard the nucleation since sufficient supercooling required for crystallization will bring temperatures close to the glassy regions.

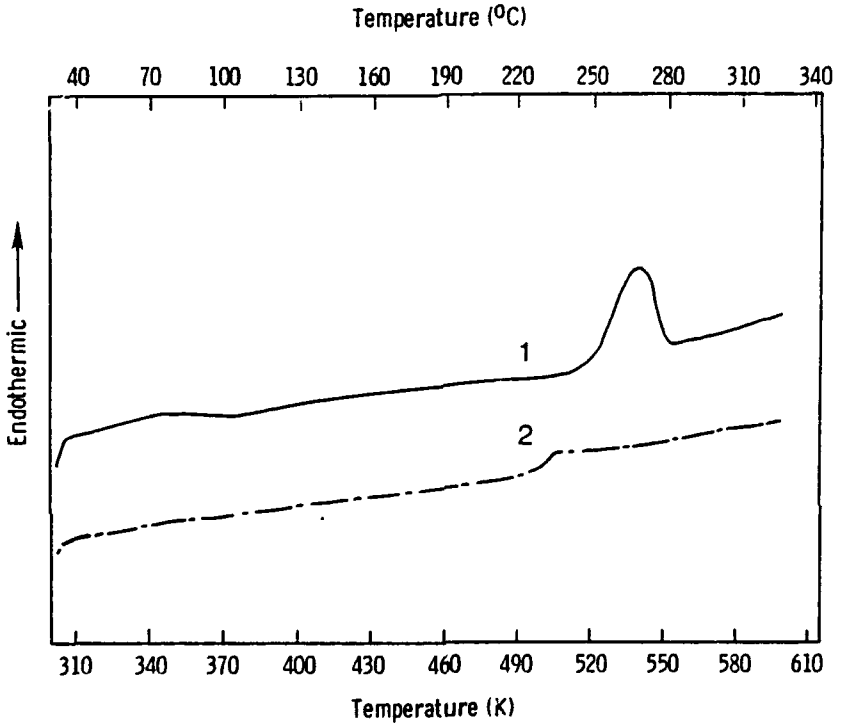

Figure 1. DSC thermograms for a typical methylene chloride-treated Ultem 5001 specimen: (1) first heating scan; (2) second heating scan.

Our first attempt to separate the melting transition from the glass transition was carried out by annealing solvent-treated specimens at the peak of the melt temperature for 10 minutes (see Curve 1 of Figure 2). The rationale is that annealing at the peak temperature, as is well known for crystalline polymers, will first melt most of the less-than-perfect crystallites. However, some of the highest melting crystals remain to promote further growth upon annealing eventually forming larger or more perfect crystallites. Consequently, the resultant microstructure after annealing will display a shift of the peak to a higher temperature. Curve 2 of Figure 2 shows a sharper melting peak, at 280°C which was obtained in the subsequent heating scan of the annealed sample. As expected, the melt temperature was higher than the original broad endotherm, 265°C, for the unannealed Ultem 5001 specimens. Again, the endothermic peak disappeared on the reheating scan (see Curve 3 in Figure 2) once the sample was heated above the melt temperature.

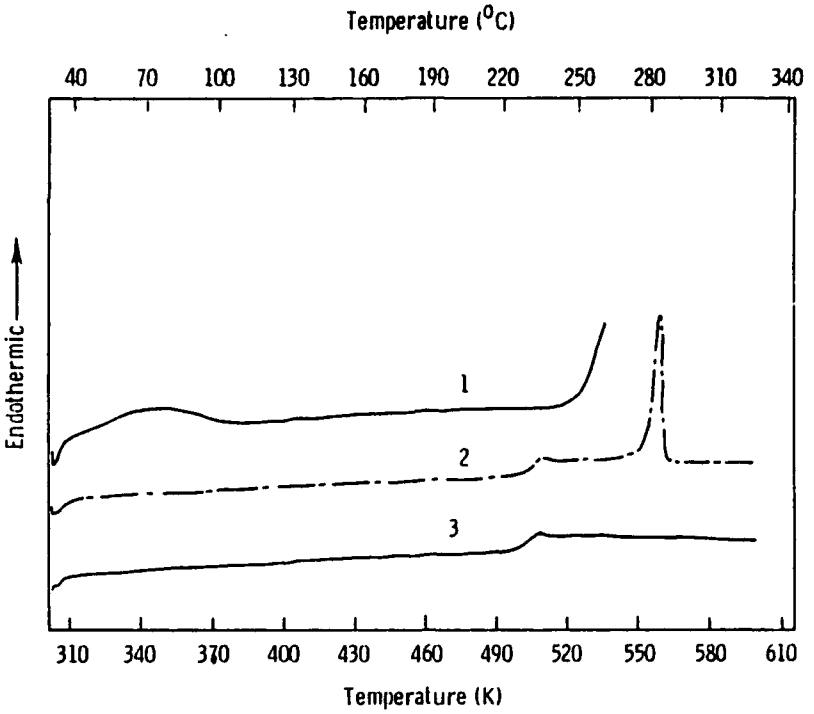

Figure 2. DSC thermograms of an annealed Ultem 5001 specimen after solvent exposure: (1) first heating scan to set the anneal temperature; (2) a reheating scan right after annealing; and (3) second reheating scan after annealing.

Attempts to further enhance crystal growth were carried out by annealing solvent-treated polyetherimide specimens at the various temperatures, as listed in Table 1. Each annealing treatment at the respective temperature required a separate film specimen. Furthermore, the procedure was carried out in a stepwise fashion; i.e., the sample at 278°C was first annealed at 248°C, followed by 258°C, 268°C, and finally at 278°C for 30 minutes at each temperature. This was required since the seed crystallites would otherwise disappear if the specimens had been heated directly to the final high annealing temperature.

Table 1. MELT TEMPERATURE AND ENTHALPY OF FUSION FOR ANNEALED ULTEM 5001

		Annealed 1/2 Hour		Annealed 3 Hours		Annealed 19 Hours	
T_{anneal}		T_{melt}	Enthalpy	T_{melt}	Enthalpy	T_{melt}	Enthalpy
°C	°K	°C	J/g	°C	J/g	°C	J/g
248	521	271	20.5	----	----	----	----
258	531	278	17.4	----	----	----	----
268	541	286	13.3	----	----	----	----
278	551	295	4.0	----	----	----	----
287	560	303	0.6	305/317	3.8	310/320	12.6
297	570	310	0.3	315/321	2.0	319/326	11.5
307	580	----	----	324	0.2	330	5.8

Figure 3 gives the DSC results which shows that the melt temperature of every melting endotherm is higher than the respective annealing temperature. The melt temperature determined after annealing for 30 minutes increased progressively as the annealing temperature increased. However, the glass transition temperature was constant at 230°C for all the annealed specimens. Table 1 summarizes the melt temperature as well as the enthalpy of fusion.

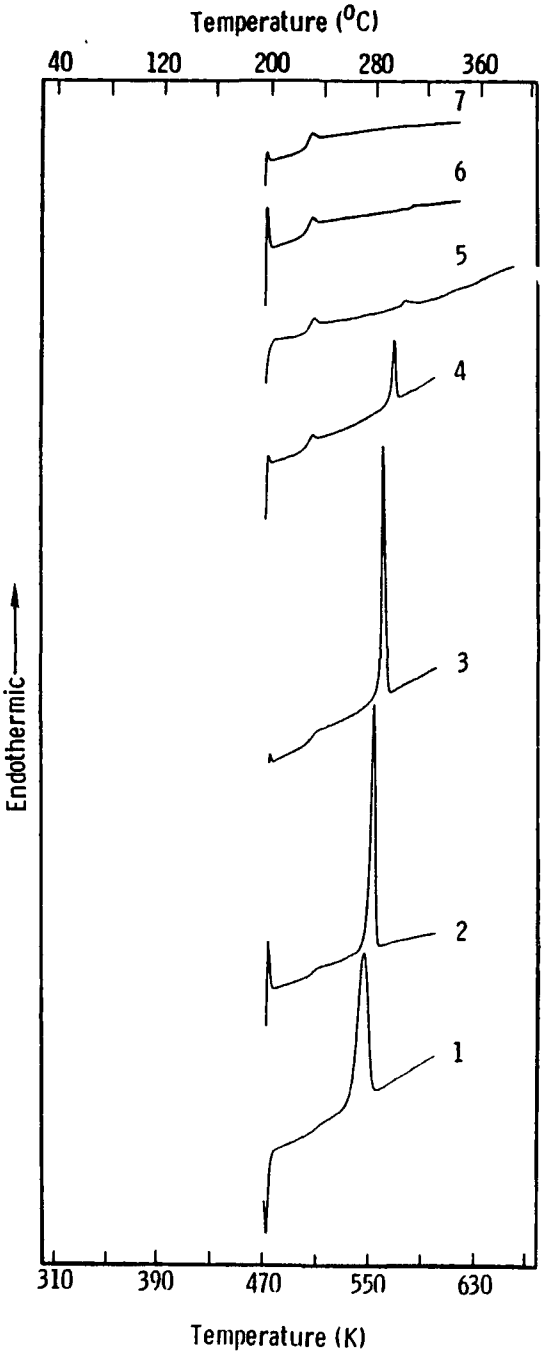

Figure 3. DSC scans of solvent-treated Ultem 5001 specimens annealed at various temperatures for 30 minutes: (1) 248°C (521°K); (2) 258°C (531°K); (3) 268°C (541°K); (4) 278°C (551°K); (5) 287°C (560°K) (6) 297°C (570°K); (7) 307°C (580°K).

The enthalpy of fusion per gram of sample is dependent upon the degree of crystallization and the degree of perfection of the existing crystal content. This was determined by the area under the endothermic peak which decreased moderately as the annealing temperature increased. Such a decrease in enthalpy of fusion can be attributed to the reduction in the recrystallization rate associated with the decrease in the degree of supercooling as the annealing temperature approaches the true melting temperature. However, the reduced enthalpy of fusion (per gram of polymer) does not necessarily suggest a reduction in the enthalpy of fusion per gram of crystallite with an increase in the annealing temperature. The latter will be elaborated with the X-ray diffraction data in the X-ray Measurements Section.

The reduction in apparent enthalpy of fusion is especially pronounced for the specimens annealed at temperatures exceeding 287°C for 30 minutes, in which only very small endotherms were noticed in the DSC thermograms, as shown in Curves 5, 6, and 7 in Figure 3. Such annealing treatments of the initially solvent crystallized samples actually proceeded at temperatures above the temperature range which was associated with the melting endotherm of Curve 1 in Figure 1.

Extended annealing was then carried out at 287°C, 297°C, and 307°C for time intervals of three hours and 19 hours, respectively, to increase crystal growth under conditions in which supercooling was relatively small. As described earlier, individual solvent-contacted samples were used for each annealing treatment, and all the samples were brought up to their final annealing temperatures in a stepwise fashion with 30 minute intermediate annealing times. Figure 4 shows the DSC thermogram obtained for the annealing treatment at 287°C. Instead of a single melting peak, there is now either a peak with a doublet or a peak with a shoulder. Temperatures of the melting peaks or the shoulder and melting peak were higher than the respective annealing temperature and it increased as the residence time at each annealing temperature increased (see Table 1). A significant increase in enthalpy of fusion (per gram of sample) also occurred as annealing time increased.

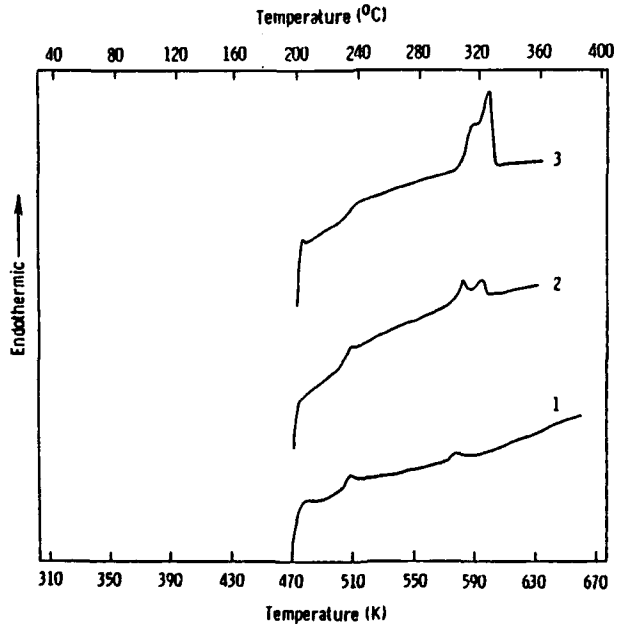

Figure 4. DSC thermograms of methylene chloride-treated specimens annealed at 287°C (560°K) and as a function of time: (1) one-half hour; (2) three hours; (3) 19 hours.

With annealing at 307°C, little crystallization occurs at three hours, as shown in Figure 5. However, when annealing was extended to 19 hours, crystallization was obtained, but only to a small extent. This can be due to either small supercooling (resulting in unfavorable crystallization kinetics) or insufficient crystal sites for further growth; therefore, an extended holding time would be needed for those samples annealed at these higher temperatures.

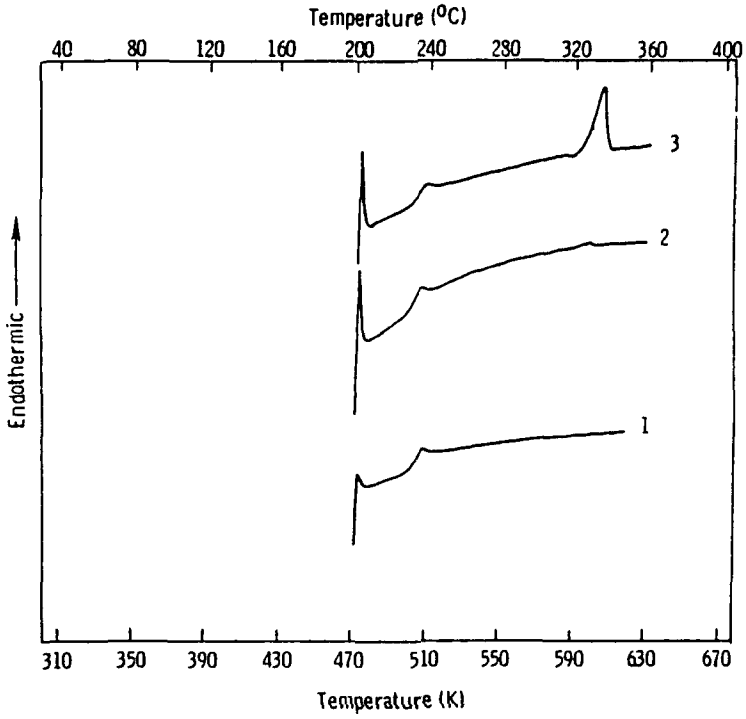

Figure 5. DSC thermograms of methylene chloride-treated specimens annealed at 307°C (580°K) and as a function of time: (1) one-half hour; (2) three hours; (3) 19 hours.

An estimate of the equilibrium melt temperature was determined using the Hoffman-Weeks[24] approach. In this method, crystallization experiments are carried out at several temperatures and values of the experimentally determined melt temperature, T_m, are plotted against the respective annealing temperature T_c. The extrapolation of T_m versus T_c to intersect with the line of $T_m = T_c$ leads to the determination of an equilibrium melt temperature for the theoretical perfect polymer crystal. Figure 6 shows an apparent equilibrium melt temperature of 369°C, based upon samples annealed for 30 minutes. Limited data obtained for the extended annealing experiments are also included in Figure 6 for comparison.

Experiments on the exposure to another chlorine containing solvent, chloroform, were also examined briefly. While instantaneous crystallization was observed with methylene chloride, Ultem 5001 film first swelled and then dissolved completely in chloroform. As chloroform was removed, the dried polyetherimide film became opaque. Figure 7 shows a broad endotherm for the chloroform-treated specimen (see Curve 1 of Figure 1). However, a distinct melting peak at 283°C was observed after annealing at the peak temperature (see Curve 4 of Figure 4). Thus, although different crystallization behavior was seen in these two chlorine-containing solvents, similar glass transition temperatures and melting endotherms were obtained.

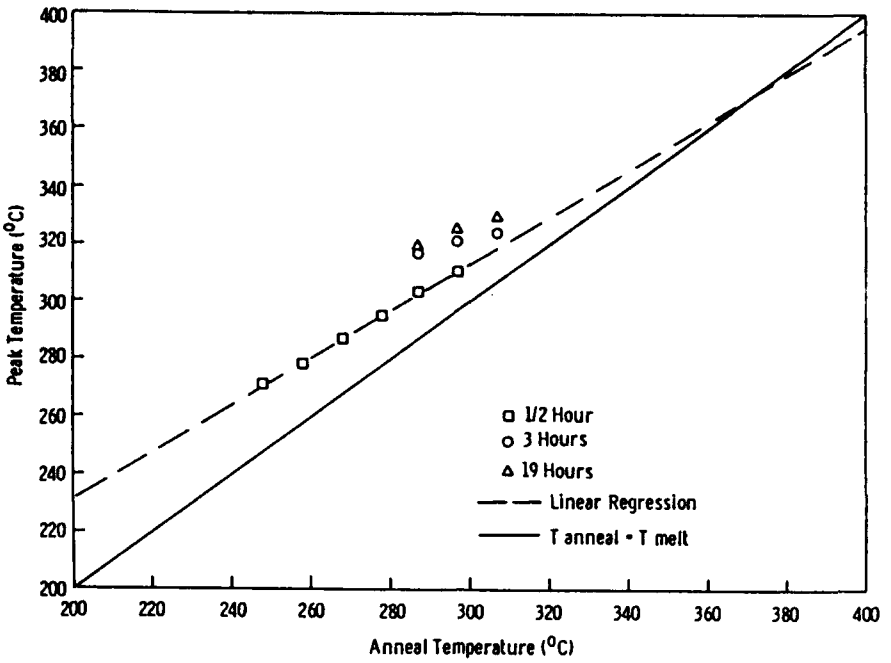

Figure 6. Plot of melt temperature versus anneal temperature for methylene chloride treated specimens annealed as a function of time: (□) one-half hour; (O) three hours; (Δ) 19 hours; (– –) linear regression of the data obtained by annealing for one-half hour; (—) $T_{anneal} = T_m$ -lt.

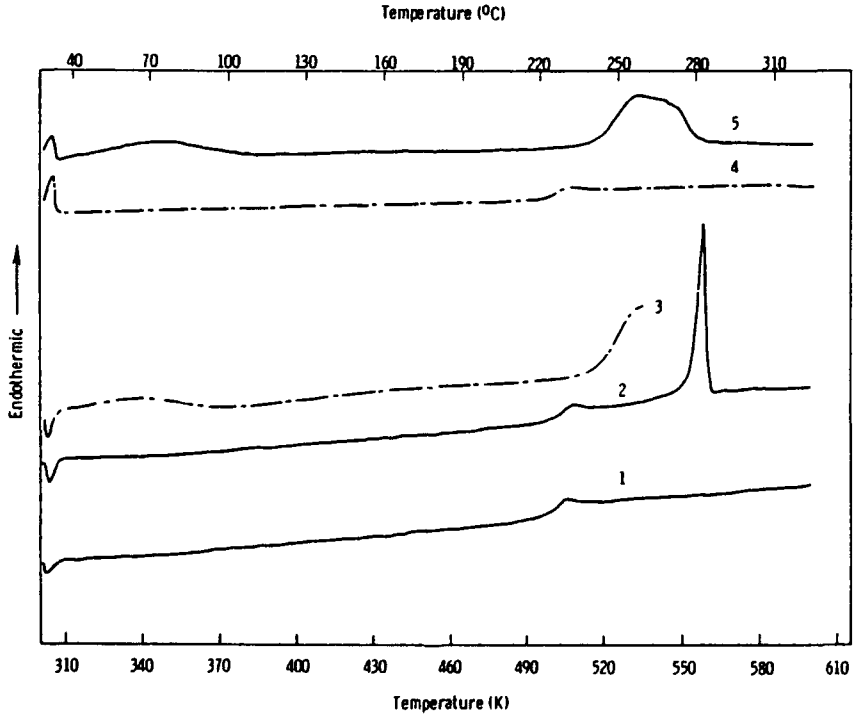

Figure 7. DSC thermograms for typical chloroform-treated Ultem 5001 film specimens: (1) first heating scan; (2) second heating scan; (3) first heating scan of another solvent-treated specimen to set the anneal temperature; (4) a reheating scan right after annealing; (5) second reheating scan after annealing.

X-Ray Measurements

To clarify observed DSC results, X-ray diffraction patterns were run at room temperature (25°C) on specimens removed from the DSC pans. In these data, three different types of diffraction patterns appeared, typified by those shown in Figure 8. The first type of pattern, as shown in Figure 8a, is totally amorphous showing a broad halo peaking near $2\theta = 17^{0}$; the second type of pattern shows three crystalline peaks superimposed on the amorphous halo, as shown in Figure 8b; and the third type of pattern shows as many as five crystalline peaks, which differs in position from those of the second type, also superimposed on the amorphous halo, as shown in Figure 8c. The amorphous peak was always present but the presence or absence, intensities, and positions of the crystalline peaks varied with annealing conditions. Table 2 shows all of the crystalline peak 2θ values and the corresponding Bragg d spacings classified into two sets:

- Three peaks at d = 5.94, 5.23, and 3.65 Å attributed to a low temperature (alpha) phase.
- Five peaks at d = 6.19, 5.51, 4.75, 4.26, and 3.81 Å attributed to a high temperature (beta) phase.

The alpha phase appears only in two patterns; samples annealed at 248°C or 258°C for one half hour, and the small number of lines observed is attributed to either crystallite imperfection, small crystallite size, or both. Any crystallinity resulting from annealing at temperatures higher than 258°C always manifested itself as the beta phase. Moreover, even at the 258°C annealing temperature the alpha phase, which appears after one half hour of annealing, transforms to the beta phase after three hours of annealing, indicating that the alpha phase is metastable relative to the beta phase even at that temperature.

The apparent X-ray crystallinity Xc was calculated from the relative intensities of crystalline and amorphous diffraction curves, based on methods originated by Matthews, Peiser, and Richards[19] and by Hermans and Weidinger.[20] Since a detailed unit cell structure has not been determined for the Ultem 5001 polyetherimide, it was not possible to apply the more rigorous methods, such as those of Ruland[21] and of Kavesh and Schultz,[22,23] for determination of crystallinity.

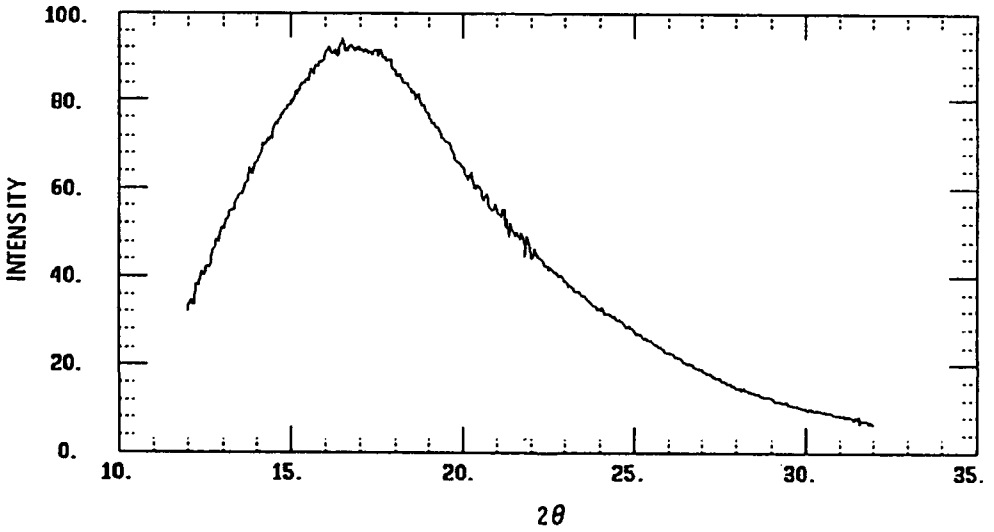

Figure 8a. WAXS patterns of methylene chloride-treated specimen annealed at 297°C (570°K) for one-half hour.

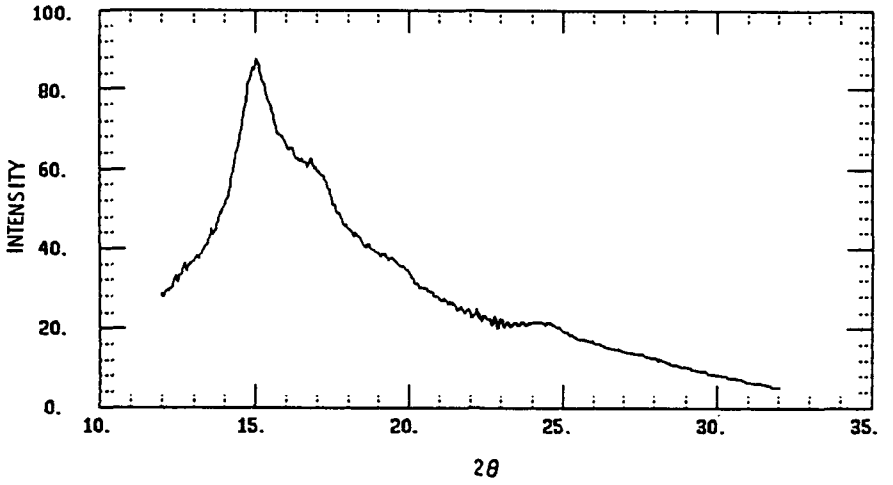

Figure 8b. WAXS patterns of methylene chloride-treated specimen annealed at 248°C (521°K) for one-half hour.

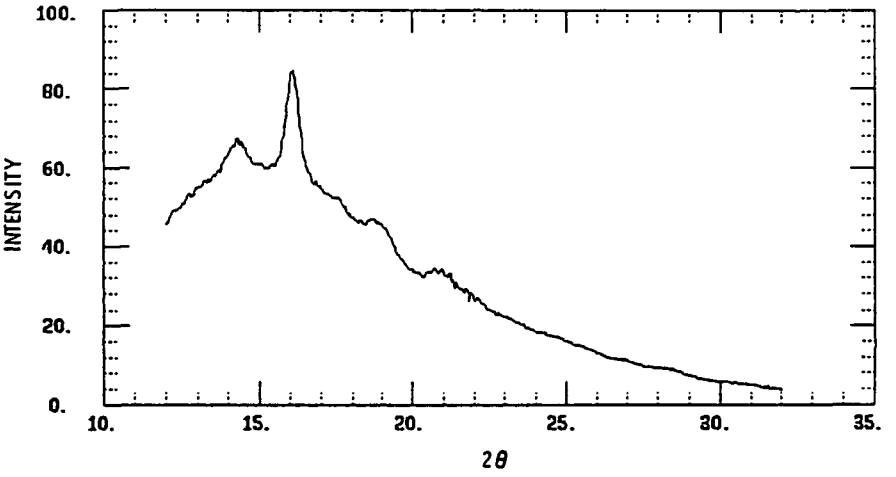

Figure 8c. WAXS patterns of methylene chloride-treated specimen annealed at 287°C (560°K) for 19 hours.

As implemented here, after background and Lorenz-polarization corrections are applied to the data between $2\theta = 12^{\circ}$ and 32°, any observed crystalline peaks are resolved mathematically from the total scattering envelope. From the peak fit parameters, the individual crystalline peak areas are summed to yield a total crystalline area of A_c; X_c is then calculated as the ratio of A_c to the total area A_t:

$$X_c = A_c / A_c \, . \qquad (1)$$

Crystallinity values determined from the X-ray diffraction patterns are included in Table 3 along with values of heat of fusion per gram of crystallite $\Delta H/X_c$. The crystallinity values are quite low, ranging from 0 to 0.083. The two highest crystallinities are observed at 0.083 and 0.070 for the alpha-phase samples obtained by crystallization for one half hour at 248°C and 258°C, respectively; the samples showing beta-phase crystallinity have, at best, X_c values up to 0.053 obtained for one half hour at 268°C. Since the X_c values have a precision of no better than, and possibly less than, two significant digits, it is anticipated that considerable

error would propagate into the $\Delta H/X_c$ values, particularly at the lower X_c values. Nonetheless, it appears that the $\Delta H/X_c$ values are quite consistent for the samples exceeding X_c = 0.030; those five samples show $\Delta H/D_c$ values of 247 J/g, 249 J/g, 251 J/g, 261 J/b, and 263 J/g. Note that two members of this group are alpha-phase samples and three are beta-phase samples. Evidently, the two crystalline phases have the same or quite similar heats of fusion.

Table 2. CRYSTALLINE PEAKS FOR ULTEM 5001 FOR VARIOUS ANNEALING CONDITIONS

Temperature		Time	2θ*	d	Phase	d (ave.)
(°C)	(°K)	(hrs.)	(deg.)	(Å)		(Å)
258	531	0.5	14.90_8	5.94_2	Alpha	5.94
248	521	0.5	14.92_5	5.93_5	Alpha	
258	531	0.5	16.93_4	5.23_6	Alpha	5.23
248	521	0.5	16.96_6	5.22_6	Alpha	
248	521	0.5	24.36_2	3.65_3	Alpha	3.65
258	531	0.5	24.43_6	3.64_3	Alpha	
287	560	19.0	14.22_2	6.22_8	Beta	
287	560	3.0	14.22_9	6.22_4	Beta	
278	551	0.5	14.34_0	6.17_6	Beta	6.19
268	541	0.5	14.37_9	6.16_0	Beta	
258	531	3.0	14.40_3	6.14_9	Beta	
307	580	19.0	15.93_8	5.56_1	Beta	
297	570	3.0	15.98_2	5.54_5	Beta	
287	560	19.0	15.99_9	5.54_0	Beta	
297	570	19.0	15.99_7	5.54_0	Beta	5.51
287	560	3.0	16.00_2	5.53_9	Beta	
258	531	3.0	16.29_2	5.44_0	Beta	
268	541	0.5	16.32_3	5.43_0	Beta	
258	531	3.0	18.26_6	4.85_7	Beta	
268	541	0.5	18.66_2	4.75_4	Beta	
307	580	19.0	18.81_3	4.71_7	Beta	4.75
297	570	19.0	18.82_2	4.71_5	Beta	
287	560	19.0	18.94_6	4.68_4	Beta	
307	580	19.0	20.75_9	4.27_9	Beta	
287	560	19.0	20.87_1	4.25_6	Beta	4.26
297	570	19.0	20.90_6	4.24_9	Beta	
258	531	3.0	23.28_3	3.82_0	Beta	
268	541	0.5	23.39_5	3.80_2	Beta	3.81
278	551	0.5	23.45_2	3.79_3	Beta	

*Peak positions have been corrected for nonlinearity of the detector.

Table 3. CRYSTALLINITY AND CRYSTALLINE HEAT OF FUSION OF ULTEM 5001 SAMPLES

Annealing Conditions			Crystallinity	Heat of Fusion	
Temperature (°C)	(°K)	Time (hrs.)	X_c by X-ray	ΔH (J/g)	$\Delta H / X_c$ (J/g)
248	521	0.5	0.083	20.5	247
258	531	0.5	0.070	17.4	249
268	541	0.5	0.053	13.3	251
278	551	0.5	0.023	4.0	174
287	560	0.5	0.000	0.6	0
297	570	0.5	0.000	0.3	0
287	560	3.0	0.022	3.8	173
287	560	19.0	0.048	12.6	263
297	570	3.0	0.010	2.0	200
297	570	19.0	0.044	11.5	261
307	580	3.0	0.000	0.2	0
307	580	19.0	0.030	5.8	193

CONCLUSIONS

Although thermal crystallization has not been achieved in Ultem 5001 polyetherimide, a rapid nucleation for crystal growth can be easily induced by methylene chloride exposure. As a result, an initially ductile amorphous polyetherimide is observed to embrittle. DSC data notes that the melt temperature increases progressively with an increase in the annealing temperature. This suggests that crystallization at higher temperatures can be achieved through careful stepwise treatments. The extrapolation leads to an apparent equilibrium melting temperature of 369°C, based upon measurements of samples annealed for 30 minutes. Two distinct crystalline phases, a low temperature (alpha) and a high temperature (beta) phase, were observed by X-ray diffraction. Crystallinity values were quite low, suggesting the profound effects of polymer viscosity, as well as the small increment between T_g and T_m in hindering crystallization. By combining DSC and X-ray results, values of the heat of fusion per gram of crystallite are consistent with a range 247 J/g to 261 J/g for the samples of higher crystallinity. The limited experiments in chloroform indicate that the crystallization behavior can be different in other solvents; therefore, it would be of interest to explore the effect of solvent, or vapor type, on the crystallization of Ultem 5001 polyetherimide and thermal stability of the induced crystals.

APPENDIX. X-RAY INTENSITY CALCULATIONS

The data were corrected on a VAX (TM Digital Equipment Corporation) 11/730 computer for background, using the cellophane tape blank patterns, and the Lorenz-polarization correction factor f_{LP} was applied. This factor, which corrects for certain X-ray instrumental effects, including the polarization effects of both the monochromator diffraction and the sample diffraction, is given[17] by:

$$f_{LP} = (1 + \cos^2 2\theta / \cos^2 2\theta_m) / (\sin^2 \theta \cos \theta) \quad (A1)$$

where 2θ is the sample Bragg angle, (the independent variable) and $2\theta_m$ is the Bragg angle of the monochromator reflection, the graphite (002) reflection in this case. Note that Equation A1 used here differs from the common form given by Alexander;[17] i.e., $1/\cos^2 2\theta_m$, representing the polarization ratio of the incident beam replaces the $\cos^2 2\theta_m$ of Alexander. This results from the geometry of the Picker monochromator, where the monochromator diffraction plane is perpendicular to the sample diffraction plane, rather than parallel, as assumed by Alexander. Therefore, the incident beam has the inverse of the polarization presumed by Alexander. It should also be noted that a denominator expression in Alexander's polarization factor, which is independent of 2θ and, thus, affects all data points equally, is omitted.

The X-ray data analysis programs also include a procedure for peak curve fitting. In this method, the intensity curve for a selected range of data which includes a peak maximum is fit to a combination of a straight line baseline, and either a Gauss or Cauchy peak function given by:

$$I_{calc}(2\theta) = A_1 + A_2 \cdot 2\theta + P(2\theta,A_3,A_4,A_5) \quad (A2)$$

where the peak function P can be identified as either the Gauss function:

$$P(2\theta,A_3,A_4,A_5) = G(2\theta,A_3,A_4,A_5) =$$

$$A_3 \exp(-(4 \ln 2 \cdot (2\theta - A_4)/A_5)^2) \quad (A3)$$

or as the Cauchy function:

$$P(2\theta,A_3,A_4,A_5) = C(2\theta,A_3,A_4,A_5) = A_3 / (1 + (2(2\theta - A_4)/A_5)^2). \quad (A4)$$

In either instance, 2θ is the independent variable, while A_1 through A_5 are adjustable parameters, to wit:

A_1 is the constant (intercept) part of the baseline straight line,

A_1 is the slope of the baseline straight line,

A_3 is the maximum intensity of the peak (Gauss or Cauchy) curve,

A_4 is the peak position of the peak curve, and

A_5 is the full width at half maximum (FWHM) of the peak curve.

The Marquardt Method, as described by Press et al.,[19] is used as an iterative procedure for fitting the experimental data $I_{expt}\ 2\theta$ to the calculated function $I_{calc}\ 2\theta$. The calculation converges to yield a solution set A_1 through A_5 for the Gauss, as well as the Cauchy function; the correct solution is taken as the one with the lower value of χ^2 which is a weighted least squares parameter.

REFERENCES

1. WILKES, G. L., and PARLAPIANO, J. *Solvent and Vapor Induced Crystallization of Bisphenol-A Polycarbonate.* ACS Polym. Prepr., v. 17, 1976, p. 937-942.
2. LEGRAS, R., and MERCIER, J. P. *Crystallization of Bisphenol-A Polycarbonate. I. Melting Behavior and Equilibrium Melting Temperature of the Plasticized Polymer.* J. Polym. Sci., Polym. Phys. ed., v. 15, 1977, p. 1283-1289.
3. JONZA, J. M., and PORTER, R. S. *High-Melting Bisphenol-A Polycarbonate from Annealing of Vapor-Induced Crystals.* J. Polym. Sci., Polym. Phys. ed., v. 24, 1986, p. 2459-2472.
4. MAKAREWICZ, P. J., and WILKES, G. L. *Diffusion Studies of Poly(ethylene Terephthalate) Crystallized in Nonreactive Liquids and Vapors.* J. Polym. Sci., Polym. Phys. ed., v. 16, 1978, p. 1529-1544.
5. MAKAREWICZ, P. J., and WILKES, G. L. *Small Angle X-ray Scattering and Crystallization Kinetics of Poly(ethylene Terephthalate) Crystallized in a Liquid Environment.* J. Polym. Sci., Polym. Phys. ed., v. 16, 1978, p. 1559-1582.
6. BERGER, L. L. *Solvent-Induced Embrittlement in a Crystallizable Polyarylate.* J. Polym. Sci., Polym. Phys. ed., v. 27, 1989, p. 1629-1647.
7. HOU, T. H., BAI, J. M., and ST. CLAIR, T. L. *Semicrystalline Polyimidesulfone Powders, in "Polyimides: Materials, Chemistry, and Characterization." C. Feger, M. M. Khojasteh, and J. E. McGrath, eds., Elsevier, Amsterdam, 1989, p. 169-191.*
8. NELSON, K. M., SEFERIS, J. C., and ZACHMANN, H. G. *Determination of Solvent-Induced Crystallization in Polyetherimide Matrix Composites by Wide Angle X-ray Scattering.* 34th Intl. SAMPE Symp. Proc., v. 34, 1989, p. 69-72.
9. AVAKIAN, P., GARDNER, K. H., and MATHESON, R. R., Jr. *A Comment on Crystallization in PEKK and PEEK Resins.* J. Polym. Sci., Polym. Lett. ed., v. 28, 1990, p. 243-246.
10. WANG, J., DIBENEDETTO, A. T., JOHNSON, J. F., HUANG, S. J., and CERCENA, J. L. *Solvent-Induced Crystallization of Aromatic Polyimid.* Polymer, v. 30, 1989, p. 718-721.
11. HOU, T. H., WAKELYN, N. T., and ST. CLAIR, T. L. *Investigation of Crystalline Changes in LaRC-TPI Powders.* J. Appl. Polym. Sci., v. 36, 1988, p. 1731-1739.
12. HOU, T. H., BAI, J. M., and ST. CLAIR, T. L. *Polymerization and Crystallization Behavior of a LaRC-TPI Powder.* J. Appl. Polym. Sci., v. 36, 1988, p. 321-333.
13. BURKS, H. D., ST. CLAIR, T. L., and GAUTREAUX, C. R. *Effects of Thermal History on the Rheological Properties of LaRC-TP in "Polyimides: Materials, Chemistry, and Characterization."* C. Feger, M. M. Khojasteh, and J. E. McGrath, eds., Elsevier, Amsterdam, 1989, p. 613-624.
14. PRATT, J. R., ST. CLAIR, T. L., GERBER, M. K., and GAUTREAUX, C. R. *A Study of Thermal Transitions in a New Semicrystalline, Thermoplastic Polyimide in "Polyimides: Materials, Chemistry, and Chacterization."* C. Feger, M. M. Khojasteh, and J. E. McGrath, eds., Elsevier, Amsterdam, 1989, p. 193-211.
15. SERFATY, I. W. *Polyetherimide: A Versatile, Processable Thermoplastic in "Polyimides: Synthesis, Characterization, and Applications."* K. L. Mittal, ed., Plenum Press, New York, NY, 1984, p. 149-161.
16. HSIEH, A. J., and SCHNEIDER, N. S. *Thermal Characterization of Solvent-Induces Crystallization of Aromatic Polyetherimide.* ACS Polym. Prepr., v. 31, 1990, p. 259-260.
17. ALEXANDER, L. J. *X-ray Diffraction Methods in Polymer Science.* Wiley-Interscience, New York, NY, 1969, p. 40-41.
18. PRESS, W. H., FLANNERY, B. P., TEUKOLSKY, S. A., and VETTERLING, W. T. *Numerical Recipes.* Cambridge Press, New York, NY, 1986, p. 523-528.
19. MATTHEWS, J. L., PEISER, H. S., and RICHARDS, R. B. *The X-ray Measurement of the Amorphous Content of Polythene Samples.* Acta Cryst., v. 2, 1949, p. 85-90.
20. HERMANS, P. H., and WEIDINGER, A. *Estimation of Crystallinity of Some Polymers from X-ray Intensity Measurements.* J. Polym. Sci., v. 4, 1949, p. 709-723.
21. RULAND, W. *X-ray Determination of Crystallinity and Diffuse Disorder Scattering.* Acta Cryst., v. 14, 1961, p. 1180-1185.
22. KAVESH, S., and SCHULTZ, J. M. *Lamellar and Interlamellar Structure in Melt-Crystallized Polyethylene. I. Degree of Crystallinity, Atomic Positions, Particle Size, and Lattice Disorder of the First and Second Kinds.* J. Poly. Sci., Part A2, v. 8, 1970, p. 243-276.
23. KAVESH, S., and SCHULTZ, J. M. *Meaning and Measurement of Crystallinity in Polymers: A Review.* Polym. Eng., & Sci., v. 9, 1969, p. 452-460.
24. HOFFMAN, J. D., DAVIS, G. T., and LAURITZEN, J. I. *The Rate of Crystallization of Linear Polymers with Chain Folding* in "Treatise on Solid State Chemistry." N. B. Hanay, ed., Plenum Press, New York, NY, v. 3, 1976, p. 497-614.

DISTRIBUTION LIST

No. of Copies	To
	Commander U.S. Army Chemical Research, Development, and Engineering Center Aberdeen Proving Ground, MD 21010-5423
1	ATTN: SMCCR-DDE
1	SMCCR-DDD
1	SMCCR-DDP
1	SMCCR-HV
1	SMCCR-MSI
1	SMCCR-MU
1	SMCCR-MUC
1	SMCCR-MUP
1	SMCCR-NB
1	SMCCR-OPC (B. Eckstein)
1	SMCCR-OPF
1	SMCCR-OPP
1	SMCCR-OPR
1	SMCCR-RS
1	SMCCR-RSC
1	SMCCR-RSL
1	SMCCR-RSP
1	SMCCR-RST
1	SMCCR-SF
1	SMCCR-SPS-T
1	SMCCR-ST
1	SMCCR-TDT (S. Lawhorne)
1	SMCCR-MUA (Record Copy)
	Commander U.S. Army Missile Command Redstone Scientific Information Center Redstone Arsenal, AL 35898-5241
1	ATTN: AMSMI-RD-CS-R (Document Section)
	Commander U.S. Army Missile Command Redstone Arsenal, AL 35898-5241
1	ATTN: AMSMI-ROC (Dr. B. Fowler)
	Commander U.S. Army Missile Command Redstone Arsenal, AL 35898-5500
1	ATTN: AMSMI-RGT (Mr. Maddix)
1	AMSMI-YDL, Bldg. 4505
1	AMSMI-YLP (Mr. N. C. Kattos)
	Commandant U.S. Army Chemical School Fort McClellan, AL 36205-5020
1	ATTN: ATZN-CM
1	ATZN-CM-CC
1	ATZN-CM-CS
1	ATZN-CM-CT
1	ATZN-CM-MLB
1	ATZN-CM-NC

No. of Copies	To
	Commander U.S. Army Aviation Center Fort Rucker, AL 36362-5000
1	ATTN: ATZQ-CAT-CA-M (CPT P. McCluskey)
1	ATZQ-D-MS
	Commander Naval Weapons Center China Lake, CA 93555
1	ATTN: Code 36
1	Code 366
1	Code 3554
1	Code 3653
1	Code 3656
1	Code 3664
1	Code 3893 (Dr. L. A. Mathews)
1	Code 3917 (Mr. D. V. Houwen) NWC
1	Coordinator
	Commander U.S. Army Science and Technology Center Far East Office San Francisco, CA 96328-5000
1	ATTN: AMXME-I-OP (David Baker)
	Director Defense Intelligence Agency Washington, DC 20301-6111
1	ATTN: DT-5A (Mr. C. Clark)
1	HQDA (DAMO-NCC) Washington, DC 20310-0403
1	HQDA (DAMI-FIT-S&T) Washington, DC 20310-1087
1	HQ USAF/INKL Washington, DC 20330-1550
	Commander Naval Air Systems Command Washington, DC 20361
1	ATTN: PMA 279A (B. Motsuk)
1	PMA 279C (LCDR F. Smartt)
	Commander Naval Sea Systems Command Washington, DC 20362-5101
1	ATTN: Code 55X25
	Commander Naval Research Laboratory 4555 Overlook Avenue, SW Washington, DC 20375-5000
1	ATTN: Code 2526 (Library)
1	Code 6182 (Dr. R. Taylor)

No. of Copies	To
	Commanding Officer Navy Intelligence Support Center Washington, DC 20390
1	ATTN: NISC-633 (Collateral Library)
	Commanding General Marine Corps Research, Development, and Acquisition Command Washington, DC 20380-0001
1	ATTN: Code SSC NBC
	Commander U.S. Army Armament, Munitions, and Chemical Command Rock Island, IL 61299-6000
1	ATTN: AMSMC-ASN
1	AMSMC-IMP-L
1	AMSMC-IRA
1	AMSMC-IRD-T
1	AMSMC-SFS
	Commander Naval Weapons Support Center Crane, IN 47522-5050
1	ATTN: Code 5063 (Dr. J. R. Kennedy)
	Commander U.S. Army TRADOC Independent Evaluation Directorate Fort Leavenworth, KS 66027-5130
1	ATTN: ATZL-TIE-C (Mr. C. Annett)
	Commander U.S. Army Combined Arms Center Development Activity Fort Leavenworth, KS 66027-5300
1	ATTN: ATZL-CAM-M
	Commander U.S. Army Cold Regions Research and Engineering Laboratory Hanover, NH 03755-1290
1	ATTN: CRREL-RG
	Commander U.S. Army Production Base Modernization Activity Dover, NJ 07801
1	ATTN: AMSMC-PBE-C(D)/Regber
	Commander U.S. Army Armament Research, Development and Engineering Center Picatinny Arsenal, NJ 07806-5000
1	ATTN: SMCAR-AE (S. Morrow)
1	SMCAR-AE (R. A. Trifiletti)
1	SMCAR-CCT
1	SMCAR-FSF-B
1	SMCAR-MSI
1	SMCAR-AET (Bldg. 335)

No. of Copies	To
	Director Los Alamos National Laboratory Los Alamos, NM 87545
1	ATTN: (S. Gerstl) ADAL, Mail Stop A104
	Commander/Director U.S. Army Atmospheric Sciences Laboratory White Sands Missile Range, NM 88002-5501
1	ATTN: SLCAS-AE (Dr. F. Niles)
1	SLCAS-AE-E (Dr. D. Snider)
1	SLCAS-AR (Dr. E. H. Holt)
1	SLCAS-AR-A (Dr. M. Heaps)
1	SLCAR-AR-P (Dr. C. Bruce)
1	SLCAR-AR (Dr. R. Sutherland)
	Director U.S. Army TRADOC Analysis Command White Sands Missile Range, NM 88002-5502
1	ATTN: ATOR-TSL
1	ATOR-TDB (L. Dominquez)
	Commander U.S. Army Materiel Command Science and Technology Center, Europe APO, New York, NY 09079-4734
1	ATTN: AMXMI-E-OP (Joe Crider)
	Commander U.S. Military Academy Department of Physics West Point, NY 10996-1790
1	ATTN: Major Decker
	Headquarters Wright-Patterson AFB, OH 45433-6503
1	ATTN: WRDC/FIEEC
1	ASD/AESD
1	AAMRL/HET
1	FTD-TQTR Wright-Patterson AFB, OH 45433-6508
1	WRDC/FIES/SURVIAC Wright-Patterson AFB, OH 45433-6553
1	AAMRL/TID Wright-Patterson AFB, OH 45433-6573
	Commander Naval Air Development Center Warminster, PA 18974-5000
1	ATTN: Code 60332 (D. Herbert)
	Commander U.S. Army Dugway Proving Ground Dugway, UT 84022-5010
1	ATTN: STEDP-SD (Dr. L. Salomon)

No. of Copies	To
	Commander U.S. Army Dugway Proving Ground Dugway, UT 84022-6630
1	ATTN: STEDP-SD-TA-F (Technical Library)
	U.S. Army Natick Research, Development and Engineering Center Natick, MA 01760-5015
1	ATTN: STRNC-AC
1	STRNC-UE
1	STRNC-WTS
1	STRNC-WT
1	STRNC-IC
1	STRNC-ICC
1	STRNC-IP
1	STRNC-ITP (Mr. Tassinari)
1	STRNC-YB
1	STRNC-YE
1	STRNC-YM
1	STRNC-YS
	Commander Harry Diamond Laboratories 2800 Powder Mill Road Adelphi, MD 20783-1145
1	ATTN: DELHD-RT-CB (Dr. Sztankay)
	Commander U.S. Army Laboratory Command 2800 Powder Mill Road Adelphi, MD 20783-1145
1	ATTN: AMSLC-IM-TL
1	AMSLC-CT
	Director U.S. Army Concepts Analysis Agency 8120 Woodmont Avenue Bethesda, MD 20814-2797
1	ATTN: CSCA-RQL (Dr. Helmbold)
	Director U.S. Army Human Engineering Laboratory Aberdeen Proving Ground, MD 21005-5001
1	ATTN: AMXHE-IS (Mr. Harrah)
	Commander U.S. Army Test and Evaluation Command Aberdeen Proving Ground, MD 21005-5055
1	ATTN: AMSTE-TE-F
1	AMSTE-TE-T
	Director U.S. Army Ballistic Research Laboratory Aberdeen Proving Ground, MD 21005-5066
1	ATTN: SLCBR-OD-ST (Technical Reports)
	Director U.S. Army Materiel Systems Analysis Activity Aberdeen Proving Ground, MD 21005-5071
1	ATTN: AMXSY-GC (Mr. F. Campbell)
1	AMXSY-MP (Mr. H. Cohen)

No. of Copies	To
	Commander U.S. Army Armament, Munitions, and Chemical Command Aberdeen Proving Ground, MD 21010-5423
1	ATTN: AMSMC-HO (A) (Mr. J. K. Smart)
1	AMSMC-QAC (A)
1	AMSMC-QAE (A)
	Director U.S. Army Research Office P.O. Box 12211 Research Triangle Park, NC 27709-2211
1	ATTN: SLCRO-CB (Dr. R. Ghirardelli)
1	SLCRO-GS
	Deputy Director Marine Corps Institute Arlington, VA 22222-0001
1	ATTN: NBC CD, CDD2
	Chief of Naval Research 800 N. Quincy Street Arlington, VA 22217
1	ATTN: Code 441
	Commander U.S. Army Materiel Command 5001 Eisenhower Avenue Alexandria, VA 22333-0001
1	ATTN: AMCCN
1	AMCSF-C
1	AMCLD
	Commander Defense Technical Information Center Cameron Station, Bldg. 5 5010 Duke Street Alexandria, VA 22304-6145
2	ATTN: DTIC-FDAC
	Commander Naval Surface Weapons Center Dahlgren, VA 22448
1	ATTN: Code E4311
1	Code G51 (Brumfield)
	Commander U.S. Army Foreign Science and Technology Center 220 Seventh Street, NE Charlottesville, VA 22901
3	ATTN: A1FRTC, Gerald Schlesinger, Applied Technologies Branch
	Director Aviation Applied Technology Directorate Fort Eustis, VA 23604-5577
1	ATTN: SAVRT-ALT-ASV

No. of Copies	To
	Commander U.S. Army Training and Doctrine Command Fort Monroe, VA 23651-5000
1	ATTN: ATCD-N
	Commander U.S. Army Armament, Munitions, and Chemical Command Aberdeen Proving Ground, MD 21010-5423
1	ATTN: AMSMC-QAO-C(A) (Dr. P. Patel)
	Commander U.S. Army Tank-Automotive Command Warren, MI 48090
1	ATTN: AMSTA-NR (Mr. R. Case)
1	AMSTA-RTS (Mr. A. Pacis)
1	U.S. Environmental Protection Agency Woodbridge Avenue (MS-104) Edison, NJ 08837-3679
1	ATTN: Exposure Reduction Technology Section (M. Gruenfeld)
	Director U.S. Army Materials Technology Laboratory Watertown, MA 02172-0001
2	ATTN: SLCMT-TML
3	Authors

U.S. Army Materials Technology Laboratory
Watertown, Massachusetts 02172-0001
TRANSIENT CRYSTALLIZATION OF AN AROMATIC POLYETHERIMIDE: EFFECT OF ANNEALING -
C. Richard Desper, Alex J. Hsieh, and Nathaniel S. Schneider

Technical Report MTL TR 91-1, January 1991, 17 pp-illus-tables, D/A Project: 1L161102AH42

AD____________
UNCLASSIFIED
UNLIMITED DISTRIBUTION

Key Words

Polyetherimide
Crystallization
Annealing

A systematic study using differential scanning calorimetry (DSC) has been performed on the annealing behavior of an aromatic polyetherimide (Ultem 5001). Although crystallization from the melt did not occur, crystallinity was easily induced in the presence of methylene chloride. With annealing, a sharp melt endotherm of the solvent-treated polyetherimide was observed. The melt temperature determined after annealing for 30 minutes increased progressively as the annealing temperature increased leading to an extrapolation to an apparent equilibrium melt temperature of 369°C. However, the melt temperature, as well as crystallinity, increased with the increase of the residence time at each annealing temperature. X-ray diffraction data revealed two distinct crystalline phases: a low temperature (alpha) phase obtained by crystallization for one-half hour at 248°C and 258°C, and a high temperature (beta) phase obtained at 258°C for three hours, or exceeding 258°C. Values of heat of fusion per gram of crystallite were consistent with a range 247 J/g to 261 J/g for the samples of higher crystallinity.

U.S. Army Materials Technology Laboratory
Watertown, Massachusetts 02172-0001
TRANSIENT CRYSTALLIZATION OF AN AROMATIC POLYETHERIMIDE: EFFECT OF ANNEALING -
C. Richard Desper, Alex J. Hsieh, and Nathaniel S. Schneider

Technical Report MTL TR 91-1, January 1991, 17 pp-illus-tables, D/A Project: 1L161102AH42

AD____________
UNCLASSIFIED
UNLIMITED DISTRIBUTION

Key Words

Polyetherimide
Crystallization
Annealing

A systematic study using differential scanning calorimetry (DSC) has been performed on the annealing behavior of an aromatic polyetherimide (Ultem 5001). Although crystallization from the melt did not occur, crystallinity was easily induced in the presence of methylene chloride. With annealing, a sharp melt endotherm of the solvent-treated polyetherimide was observed. The melt temperature determined after annealing for 30 minutes increased progressively as the annealing temperature increased leading to an extrapolation to an apparent equilibrium melt temperature of 369°C. However, the melt temperature, as well as crystallinity, increased with the increase of the residence time at each annealing temperature. X-ray diffraction data revealed two distinct crystalline phases: a low temperature (alpha) phase obtained by crystallization for one-half hour at 248°C and 258°C, and a high temperature (beta) phase obtained at 258°C for three hours, or exceeding 258°C. Values of heat of fusion per gram of crystallite were consistent with a range 247 J/g to 261 J/g for the samples of higher crystallinity.

U.S. Army Materials Technology Laboratory
Watertown, Massachusetts 02172-0001
TRANSIENT CRYSTALLIZATION OF AN AROMATIC POLYETHERIMIDE: EFFECT OF ANNEALING -
C. Richard Desper, Alex J. Hsieh, and Nathaniel S. Schneider

Technical Report MTL TR 91-1, January 1991, 17 pp-illus-tables, D/A Project: 1L161102AH42

AD____________
UNCLASSIFIED
UNLIMITED DISTRIBUTION

Key Words

Polyetherimide
Crystallization
Annealing

A systematic study using differential scanning calorimetry (DSC) has been performed on the annealing behavior of an aromatic polyetherimide (Ultem 5001). Although crystallization from the melt did not occur, crystallinity was easily induced in the presence of methylene chloride. With annealing, a sharp melt endotherm of the solvent-treated polyetherimide was observed. The melt temperature determined after annealing for 30 minutes increased progressively as the annealing temperature increased leading to an extrapolation to an apparent equilibrium melt temperature of 369°C. However, the melt temperature, as well as crystallinity, increased with the increase of the residence time at each annealing temperature. X-ray diffraction data revealed two distinct crystalline phases: a low temperature (alpha) phase obtained by crystallization for one-half hour at 248°C and 258°C, and a high temperature (beta) phase obtained at 258°C for three hours, or exceeding 258°C. Values of heat of fusion per gram of crystallite were consistent with a range 247 J/g to 261 J/g for the samples of higher crystallinity.

U.S. Army Materials Technology Laboratory
Watertown, Massachusetts 02172-0001
TRANSIENT CRYSTALLIZATION OF AN AROMATIC POLYETHERIMIDE: EFFECT OF ANNEALING -
C. Richard Desper, Alex J. Hsieh, and Nathaniel S. Schneider

Technical Report MTL TR 91-1, January 1991, 17 pp-illus-tables, D/A Project: 1L161102AH42

AD____________
UNCLASSIFIED
UNLIMITED DISTRIBUTION

Key Words

Polyetherimide
Crystallization
Annealing

A systematic study using differential scanning calorimetry (DSC) has been performed on the annealing behavior of an aromatic polyetherimide (Ultem 5001). Although crystallization from the melt did not occur, crystallinity was easily induced in the presence of methylene chloride. With annealing, a sharp melt endotherm of the solvent-treated polyetherimide was observed. The melt temperature determined after annealing for 30 minutes increased progressively as the annealing temperature increased leading to an extrapolation to an apparent equilibrium melt temperature of 369°C. However, the melt temperature, as well as crystallinity, increased with the increase of the residence time at each annealing temperature. X-ray diffraction data revealed two distinct crystalline phases: a low temperature (alpha) phase obtained by crystallization for one-half hour at 248°C and 258°C, and a high temperature (beta) phase obtained at 258°C for three hours, or exceeding 258°C. Values of heat of fusion per gram of crystallite were consistent with a range 247 J/g to 261 J/g for the samples of higher crystallinity.